CERN/ISRC 75-33
29 August 1975

PROPOSAL FOR AN IMPROVEMENT OF EXPERIMENT R605 IN 1976: AN IMPROVED SET-UP TO SEARCH FOR MUON - ELECTRON COINCIDENCES AND HADRONIC STATES OF NEW PARTICLES AT THE ISR

Aachen-CERN-Harvard-Munich-Riverside Collaboration

L. Baksay
L. Baum
A. Boehm
M.M. Block(**)
F. Geradini
B. Couchman
J. Crawford
R. Glauber
J. Irion
A. Kernan
J. Layter
W. Marsh
F. Muller
B. Naroska
M. Nussbaum
A. Orkin-Lecourtois(*)
C. Rubbia
D. Schinzel
B. Shen
A. Staude
R. Voss.

ABSTRACT

The rapid development of the field of new particles motivates a revision for the second phase of experiment R605. The physics motivations remain unchanged, whilst the detecting apparatus has been improved to achieve sensitivity to a much broader class of new phenomena.

---

*) Supported by LAL - Orsay

**) Presently at Northwestern University.

FM/mk

About eight months ago we have initiated at the ISR a search for μ-e coincidences as a signature for charmed particles production and decay. So far the results are negative. However the tremendous progress obtained at SLAC and DESY on the ψ-complex which now appears in remarkable agreement with the "charmonium" hypothesis spurs new searches with improved sensitivity for "free" charmed states. A further, important, justification for searching μ-e coincidences comes from the possible observation by M. Perl and coll. at SLAC of heavy leptons pairs, each one decaying into a muon and an electron and from the observation at Fermi lab of the Drell-Yan mechanism with the correct intensity. The premises exist for direct production in proton proton collisions of pairs of heavy leptons with subsequent decay into muon-electron coincidences. Finally the cross section for ψ-production at ISR energies has been found almost 60 times larger than the one at BNL. The rate of $\psi \to e^+e^-$ in our detector is of 50/hour for $L = 10^{31}$ cm^{-2} sec^{-1}. Therefore as much as 10^4 ψ's could be collected during an effective data taking time of 200 hours. It is conceivable that production of charmed states is greatly enhanced when in association with ψ-states.

The proposal is to improve the present electron telescope.

The new electron detector is basically simpler and as yet it covers a solid angle which is about 100 times larger. Construction is modular, relatively cheap and it can be realised in a short time. If acceptance is granted soon, the turn over from R605 phase 1 to the new phase of the experiment could take place starting mid-february 1976.

The present first phase of R605 has led to three main results:

i) a persistently large electron signal down to very small transverse momenta (fig. 1) ($p_T \sim 0.3$ GeV/c).

ii) absence of strange particle (Λ, K) excess for e-associated events.

iii) absence of associated muon coincidence to the level of our background ($\mu/\pi \sim 10^{-2}$).

As pointed out in our original proposal R605, this was intended as a first phase of the research program, where the speed of construction and of operation was accepted as a trade-off for ultimate sensitivity. A second phase for a more sensitive search was proposed and approved at that time.

The present document is intended as a revision of the second phase of R605 proposed. For a detailed discussion of the physics motivations we shall refer to the R605 proposal.

The new electron telescope (Fig. 2) has a good acceptance over almost all azimuths for particles emitted between 11^{o} and 40^{o} with respect to the direction of beam 1. Therefore it extends the acceptance of the forward spectrometer which already covers angles from 1.1^{o} to 6.3^{o}. This is particulary apparent when one considers the acceptance in the rapidity variable (Fig. 3). We remark the dramatic improvement of the acceptance with respect to the present detector.

The electron telescope provides magnetic analysis for charged particles $11^{o} < \Theta < 40^{o}$. The magnetic field is generated by a simple set of air coils, arranged in order to generate a toroidal field which is zero outside the volume and varying inside it, approximately like 1/r, where r is the distance from the main axis (Fig. 4). This rather unusual field distribution has been chosen since it is the most appropriate in order to generate a constant average momentum resolution for all particles emitted over the large angular range of the telescope. A field variation proportional to 1/p matches momenta of particles at different angles to the bending power in order to give a deflection angle independent of emission angle Θ and inversely proportional to the transverse component of the momentum, $p_T = p \sin \Theta \sim pr$. The magnetic deflection is then calculated with the simple formula

$$\Theta_d = 21 \text{ m rad GeV}/p_T \quad (\Theta\text{-independent})$$

The momentum accuracy for $p_T > 0.4$ GeV/c is dominated by the error on the magnetic deflection and it is given by(*)

$$\frac{\Delta p}{p} = 0.06 \text{ GeV}^{-1} \cdot p_T$$

The main parameters of the magnet are summarized in table 1. A detailed drawing of the coil structure is shown in fig. 5. A steel insert is used to shield away the field from the vacuum pipe of beam 2. Two steel structures, coaxial with the main magnet axis, provide shielding for the residual, very small field on beam 1 and general support for the coils and the detectors. The coils are shaped to leave open a forward cone of $\sim$ 100 mrad in order not to obstruct the acceptance of the forward spectrometer. To optimize the usable area of the magnet the coils have to be very thin. We propose to make them out of aluminium plates of 2.5 cm thickness. The plates will be milled to give a spiral shaped coil of 12.5 turns. The plate is sealed on each side with a non-conducting sheet, and the cooling water flows through the groove in the aluminium plate.

There are three sets of planes of drift chambers, two in front and one behind the magnet (Fig. 2). Each plane is made up of two identical drift chamber modules, one above and the other below the beam pipe. The three chambers of a module measure the vertical displacement and the displacements along an axis 60° to the vertical.

The geometry of the chamber system (Fig. 2) is designed to approximately cover the angular region 11° to 40°. This requires for each module in plane A a sensitive area of 500 x 1300 mm^2, in plane B 800 x 2000 mm^2 and in plane C 1900 x 3800 mm^2. The detailed design of the chambers is shown in fig. 6.

(*) We shall assume the conservative value for the accuracy of ±0.6 mm for the large chambers and ±0.2 mm for the small ones.

The design of the chambers follows very closely the one developed by some of us for the neutrino experiment at Fermi lab. A drift cell is shown in fig. 7. Four anode-wires collect the electrons drifting from each track, giving a measurement of position and angle of the track with two constraints.

The double layer of anode wires eliminates the left-right ambiguity. The arrangement of the anodes together with the field shaping cathodes provides a high level of uniformity of the drift field and it guarantees the best uniformity and spatial resolution.

The gas Cerenkov counters, which fill the surface between adjacent "spokes" of the magnet, are designed on the basis of our experience to date on R605. As before, the radiator is CO_2 at atmospheric pressure giving excellent pion rejection up to 5 GeV. The mirror coating is Al with a layer of Mg F2; a fully relativistic particle should give in 1.2m a signal of $\sim$ 9 photo-electrons. The tubes used are 5" quantacons, with U.V. transmitting glass cathodes. One is used for each counter. Details of the counter are seen in fig. 2.

In order to provide for a redundant identification of electrons, in analogy of what it is done in the present set-up, we propose to have a finely subdivided hodoscope of lead-scintillator shower counters. The electron signature is then a rapid rise in the dE/dX losses after a few radiaton lengths. Tests will be performed in order to define the optimum configuration of the counter.

Finally some (6) of the 12 slots between the spokes can be filled-up with steel blocks in the place of the gas Cerenkov counter (Fig. 8). This transforms the segments into muon detectors and increases the field in the other segments. The field in the steel blocks however, is barely sufficient to determine the sign of the muons.

TABLE 1

Parameters of Magnet

1.	Number of coils		24
2.	Number of turns/coil		12.5
3.	Material		AL
4.	Cross section of coil		90 cm^2
5.	Weight of AL		∿ 2t
6.	Length		1.2 m
7.	Outer radius front		130 cm
8.	Outer radius back		220 cm
9.	Current		2000 A
10.	Power dissipation		0.5 MW
11.	Field at - $\Theta = 11^{o}$		0.3 T
12.	Inside shield 4 cm thick	iron	0.7 t
13.	Outside shield 1 cm thick	iron	1 t
14.	Beam 2 shield	iron	. 9 t

FIGURE CAPTIONS

Fig. 1. Present results on the $e^{\pm}/\pi$ ratio. All backgrounds have been substracted, except Ke_3, which is less than 10^{-4}. There is a systematic calibration error of ±10%.

Fig. 2. New Experimental Arrangement.

Fig. 3. Rapidity Acceptance of the Set-up.

Fig. 4. Schematic of Magnet Wheel Sections.

Fig. 5. Front view of the Magnet.

Fig. 6. Module Schematic.

Fig. 7. Drift Cell -- Detail.

Fig. 8. Proposed Electron-Muon Detector.

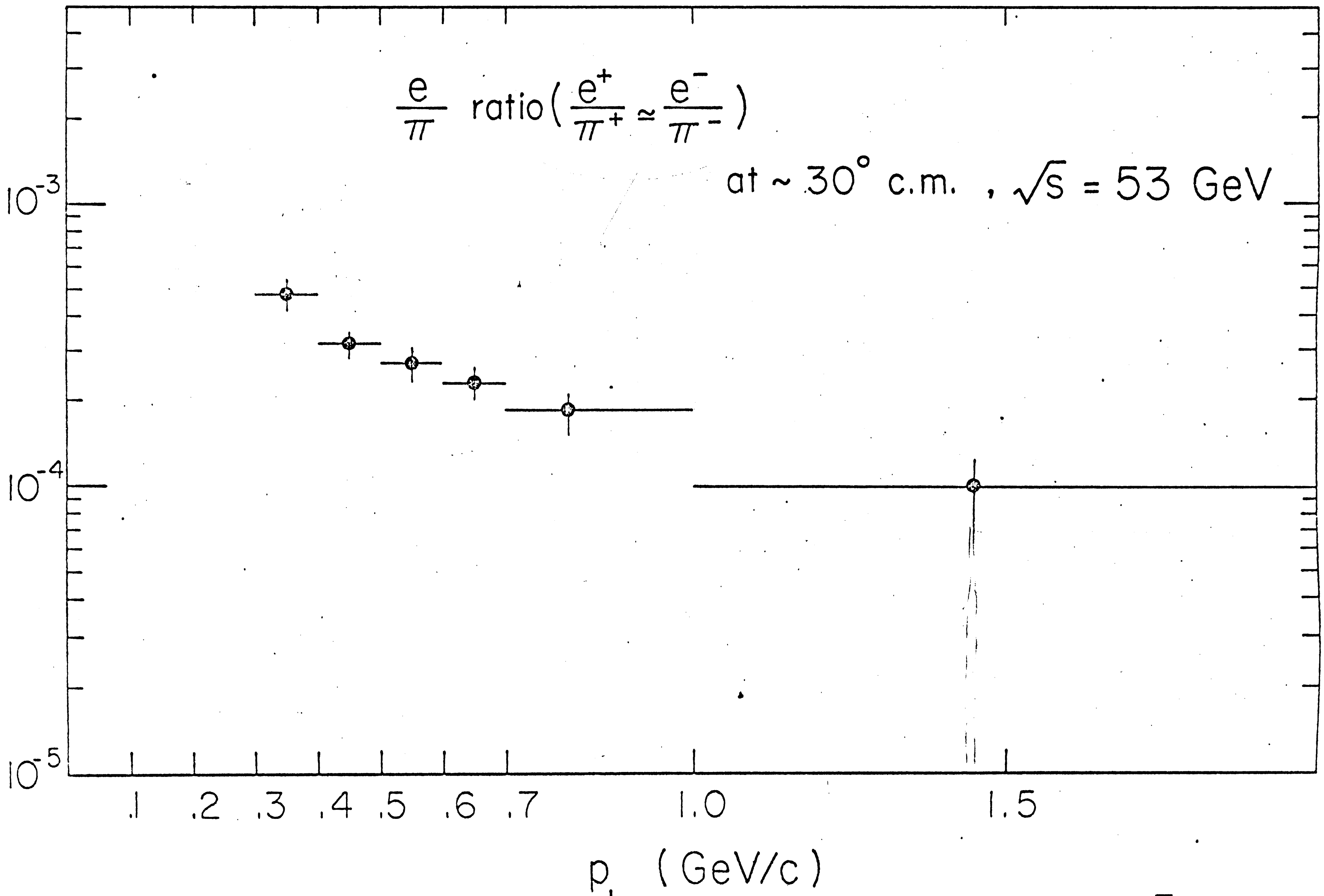

Fig. 1

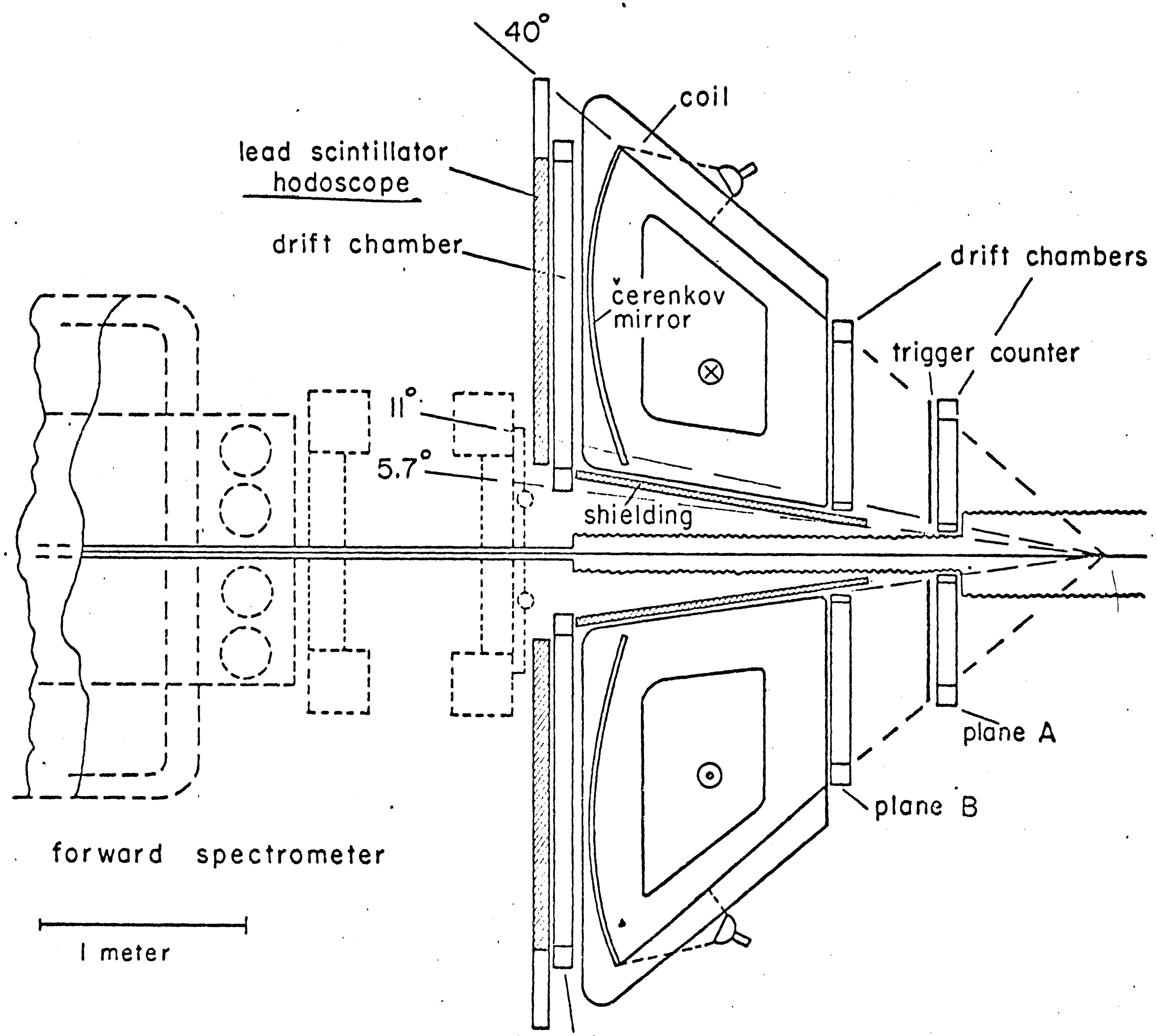
40°
coil
lead scintillator
hodoscope
drift chamber
drift chambers
čerenkov
mirror
trigger counter
11°
5.7°
shielding
plane A
plane B
plane C
forward spectrometer
1 meter

FIG. 2

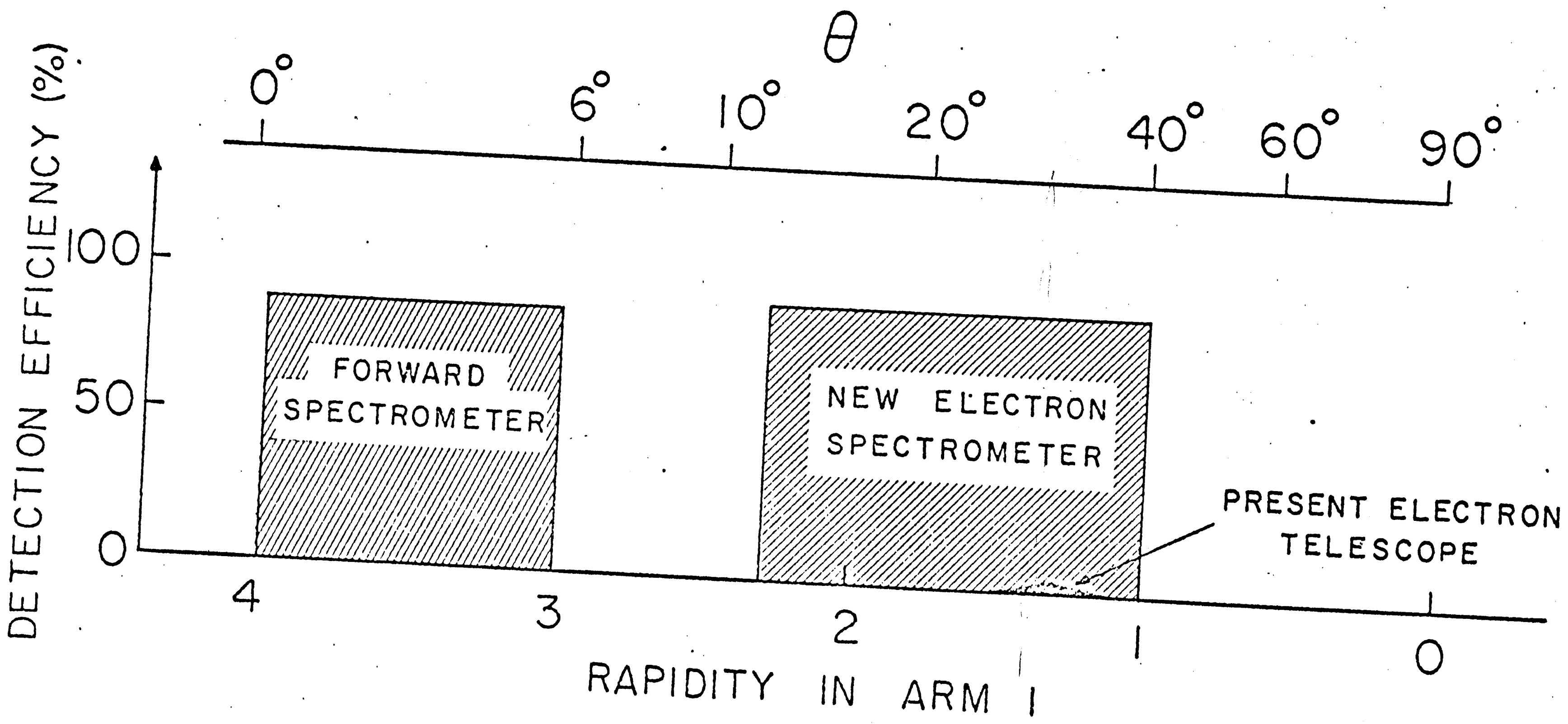
θ
0°
6°
10°
20°
40°
60°
90°
DETECTION EFFICIENCY (%)
100
50
0
FORWARD
SPECTROMETER
NEW ELECTRON
SPECTROMETER
PRESENT ELECTRON
TELESCOPE
4
3
2
1
0
RAPIDITY IN ARM I

FIG. 3

LAMP-SHADE MAGNET (L.S.M.)

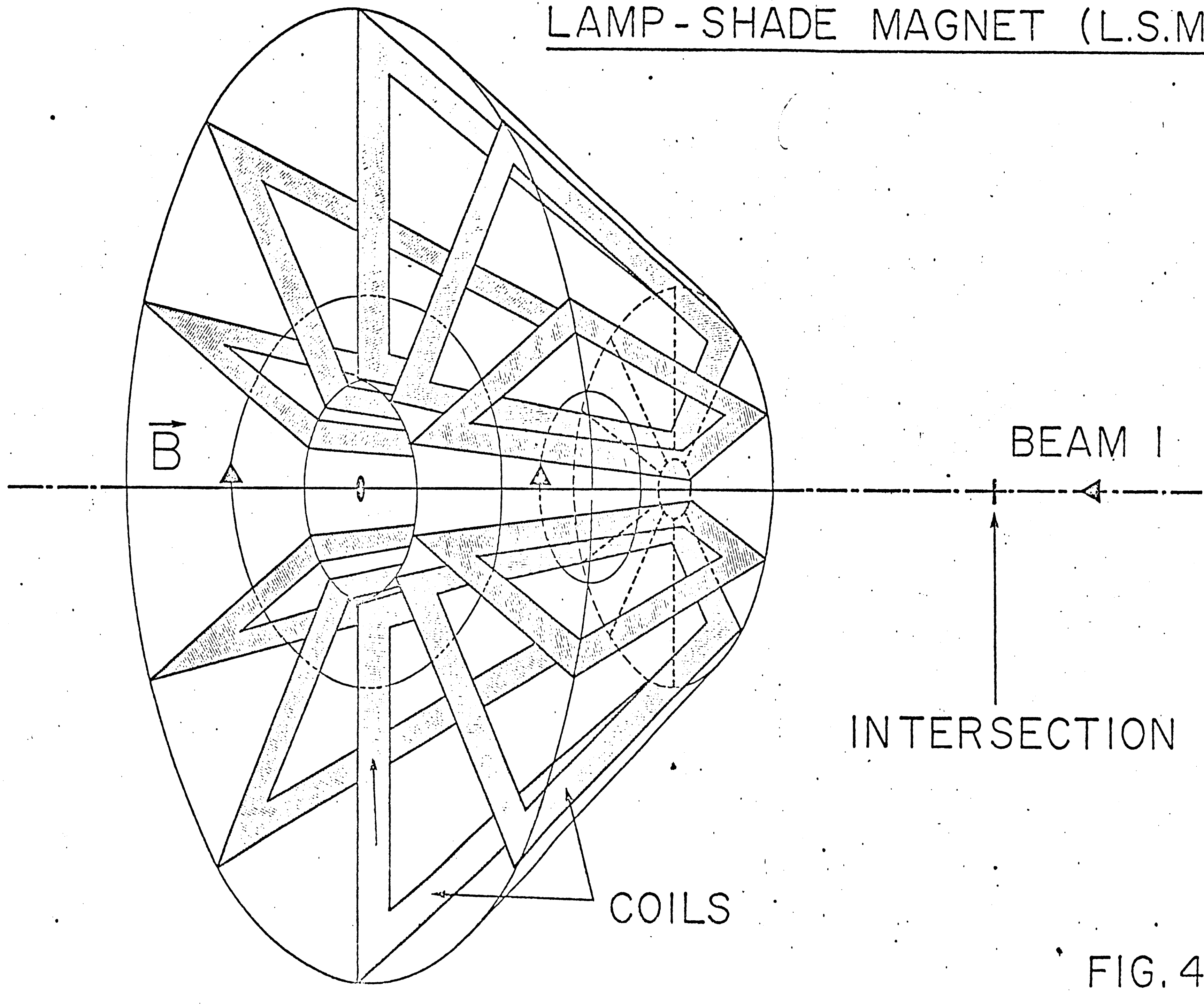

FIG. 4

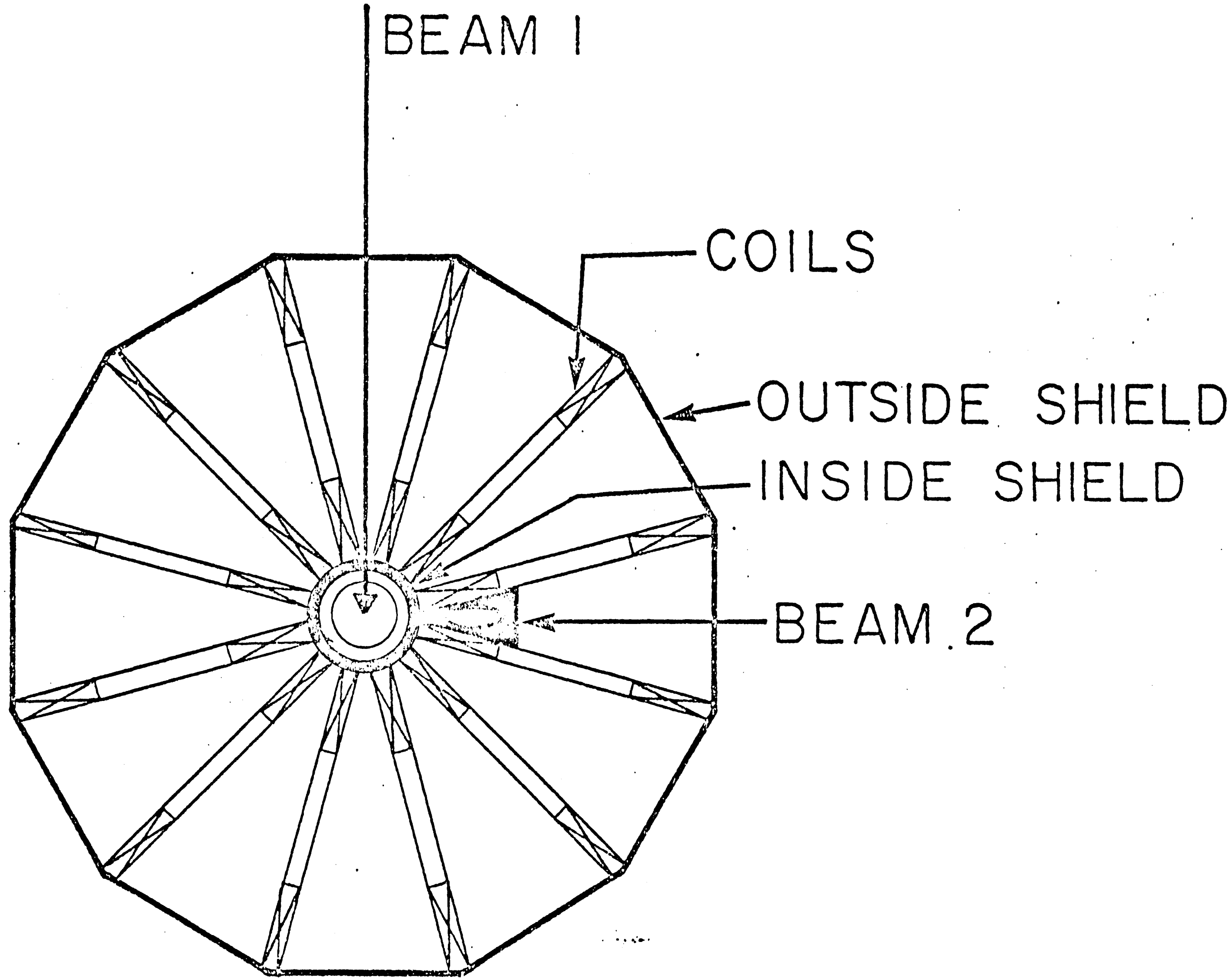

FRONT VIEW OF MAGNET

FIG. 5

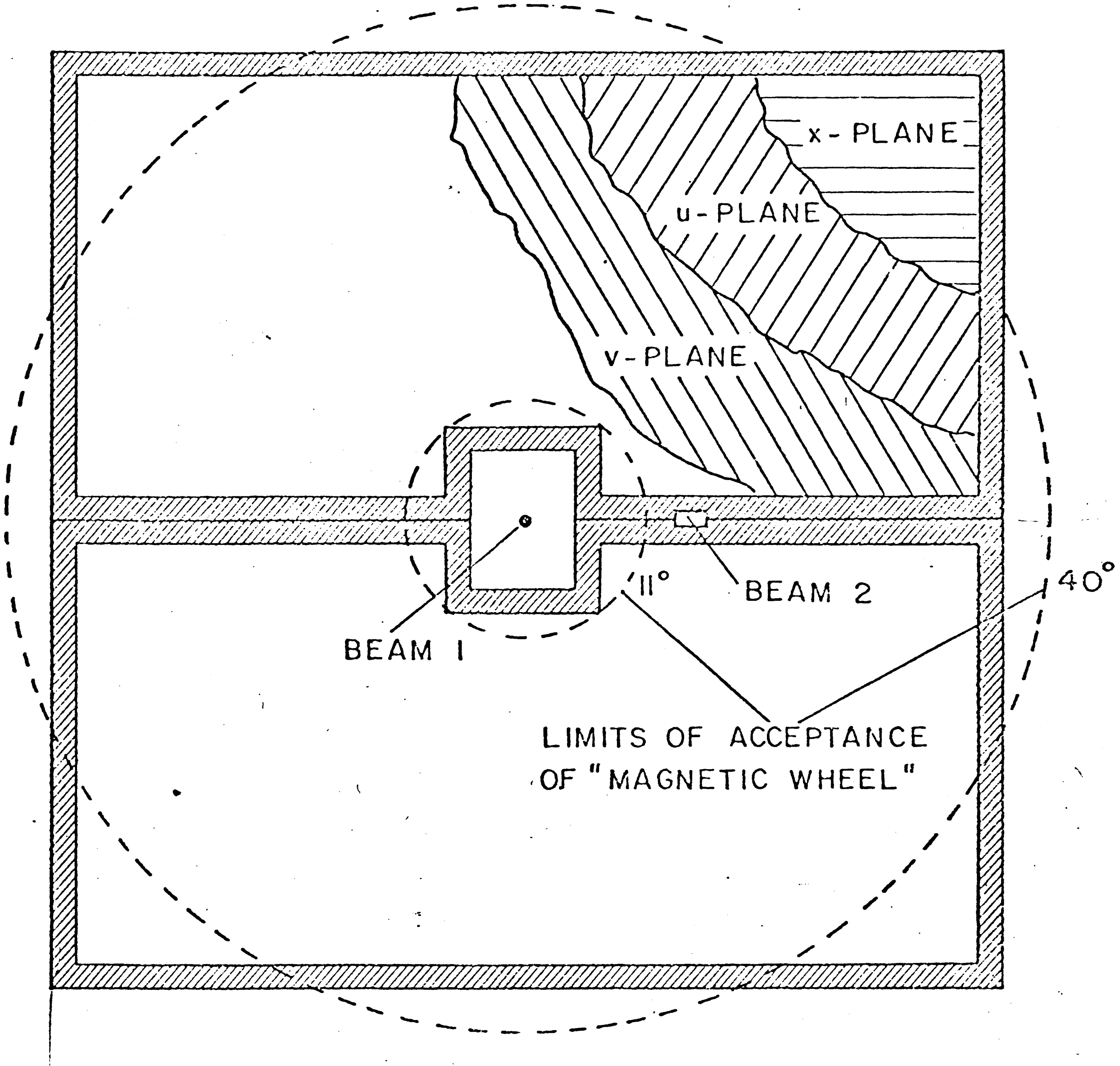

DRIFTCHAMBER MODULES BEHIND
MAGNETIC WHEEL

FIG. 6

DRIFT-CELL OF CHAMBER

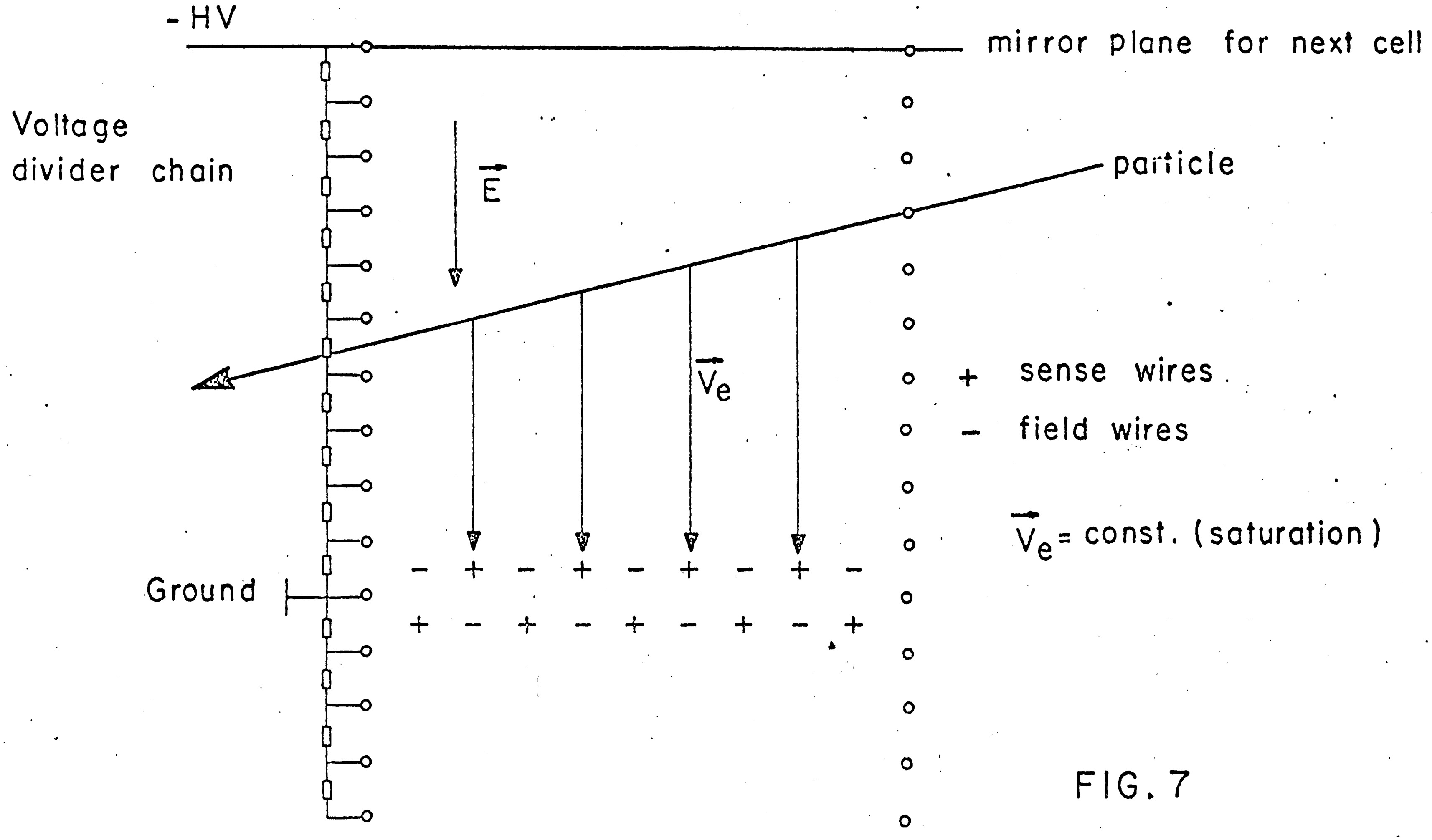

FIG. 7

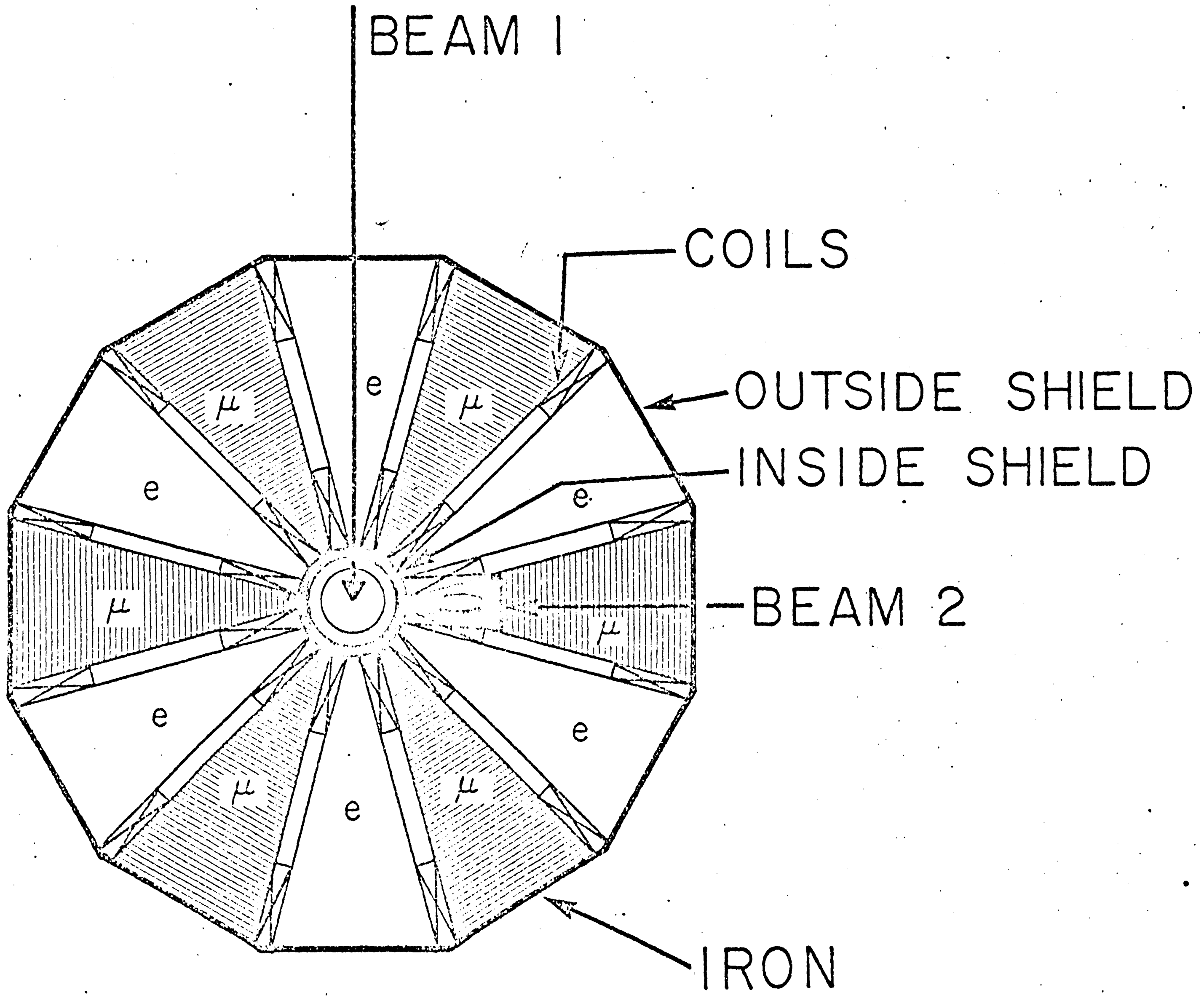

FRONT VIEW OF MAGNET